

# RADIATION TRANSPORT IN SOOTY POOL FIRES: MEASUREMENT AND ANALYSIS

by

R. S. Longenbaugh  
Division 6322 Sandia National Laboratories

L. K. Matthews  
Department of Mechanical Engineering  
New Mexico State University  
Las Cruces, New Mexico 88003

## ABSTRACT

The characterization of the heat transfer environment within a sooty pool fire has gained interest over the past few years due to the concern of transporting sensitive materials over large distances. Several investigators<sup>1,2,3</sup> have shown that the heat transfer environment within a sooty pool fire is due predominantly to radiative transfer. This report summarizes some of the work performed<sup>4</sup> by the authors on characterizing the radiation transport in a sooty pool fire.

Radiative fluxes were measured and used to estimate the absorption coefficient in the sooty pool fire as well as the radiative field environment. Transpiration heat flux gages<sup>5</sup> were modified to function in the severe environment that exists within the fire. These measurements coupled with the techniques of nonlinear parameter estimation and the equation of radiative transfer<sup>6</sup> yielded mean absorption coefficients of 0.006/cm to 0.017/cm for the combustion of liquid JP-4 fuel.

## INTRODUCTION

In recent years an increasing interest in the effects of fires on shipping containers carrying radioactive materials has spurred a renewed effort to investigate the possible hazards that might exist. This interest is brought about by Part 71, Title 10, of the code of Federal Regulations (10 CFR 71)<sup>7</sup>, which specifies a hypothetical accident in which the shipping cask must survive and still provide containment. The Transportation Technology Center and the Thermal Test and Analysis group at Sandia National Laboratories have been concerned with the thermal effects of a container engulfed in a naturally occurring sooty pool fire. "Naturally occurring" means the fire naturally entrains air for the combustion process. This causes the fire to become oxygen-starved and leads to the formation of large soot deposits. The pool-fire was chosen to represent the thermal environment specified by 10 CFR 71. In order for Sandia Laboratories to develop containers for carrying radioactive materials, the physical processes that exist within the sooty pool fire must be better understood.

It is the objective of this study to investigate the significance of radiative transfer within a sooty pool fire. This is brought about because in a large scale pool fire (large scale usually means fires with a pool diameter greater than 0.2-0.3 meters<sup>1</sup>, radiation is the dominant heat transfer mode<sup>1,2,3</sup>. On the average, the ratio of radiation to convection is approximately four to one<sup>2,8</sup>. It was determined in this analysis that because of the large soot concentrations within the sooty pool fire, the radiation characteristics of the pool fire are absorption dominant<sup>4</sup>. This is also shown by others<sup>1,9</sup> or at least discussed.

Nonlinear parameter estimation (Ref. (10)) is used to estimate radiation parameters such as the absorption coefficient and the extinction coefficient. To obtain the parameter estimates, a computer model was developed at New Mexico State University (NMSU). This model was used in conjunction with experimental data obtained from the Thermal Test and Analysis group in the form of flame temperatures and radiative heat flux distribution.

The topics to be presented in this paper will include the theoretical modeling of radiative heat transfer within a pool fire, and experimental methods used to help determine heat transfer parameters within a fire.

## MODEL DEVELOPMENT

Theoretical modeling of transient radiation heat transfer within an emitting, absorbing, and possibly scattering medium is an extremely complex problem requiring different methods and assumptions. Some of the main difficulties encountered in modeling a pool fire are extreme temperature distributions, non-homogeneous combustion products, soot concentrations, and turbulence within the fire<sup>6</sup>. Quantifying the effect of soot on the flame radiation requires knowledge of the soot distribution, the radiation properties of the soot, and the local soot temperature<sup>6</sup>.

The general equation of radiative transfer<sup>6</sup> that models the physical processes within a sooty pool fire is given below:

$$\mu \frac{dI}{dx} = -\kappa I + \alpha n^2 I_b + \frac{\sigma_s}{4\pi} \int_{\mu'} \int_{\phi'} I(x, \mu', \phi') \Phi(\mu', \phi' \rightarrow \mu, \phi) d\mu' d\phi' \quad \text{Eq. (1)}$$

This equation describes the absorption, emission, and scattering processes that exist within a sooty pool fire for the case of elastic, independent, anisotropic scattering.

The model to be considered is derived from Eq. (1) by making the following assumptions:

1. In-scattering can be neglected.
2. A one-dimensional radiation field exists.
3. The index of refraction of the fire is the same as that of air and is equal to one.
4. The radiation properties of the fire are gray.

The above assumptions are made primarily because of the lack of information. However, many authors<sup>1,2,3</sup> have made the same type of assumptions. For a more detailed discussion of these assumptions, see Reference 4. With these assumptions, Eq. (1) simplifies to the following non-homogeneous, linear, first-order differential equation:

$$\frac{dI}{dx} = -\kappa I + \alpha n^2 I_b \quad \text{Eq. (2)}$$

with the corresponding boundary condition of

$$I(0) = I_0 \quad \text{Eq. (3)}$$

The first term on the right-hand side in Eq. (2) represents the attenuation of energy by extinction due to absorption and scattering. The second term in Eq. (2) represents the local emission of thermal radiation. It should be noted that Eq. (2) is valid for the intensity of a continuous homogeneous medium along a fixed direction only.

To solve Eq. (2) for  $I$ , the temperature distribution and the boundary condition must be known. Both may be determined experimentally. In contrast, intensity cannot be measured and must be determined indirectly from measurements of radiative flux. Therefore the intensity can be found by using the following relationship:

$$q = 2\pi \int_0^{\pi/2} I \mu d\mu \quad \text{Eq. (4)}$$

By assuming that the intensity is uniform in all directions, Eq. (4) can be integrated and the following equation results:

$$q = \pi I \quad \text{Eq. (5)}$$

Once an estimate of the extinction coefficient is known, one can determine the optical thickness of the fire. The extinction coefficient is assumed to be independent of temperature, pressure, species concentration, and wavelength. This assumption was made due to the lack of information of  $\kappa$ 's dependence on the above properties. From the definition of optical thickness<sup>6</sup>,

$$\tau(x) = \int_0^x \kappa dx \quad \text{Eq. (6)}$$

the extinction coefficient may be brought out of the integral and the optical thickness then becomes

$$\tau(x) = \kappa x \quad \text{Eq. (7)}$$

Since the temperature distribution within the pool fire will not be uniform, an exact solution to

Eq. (2) would be difficult to obtain. Instead, a numerical technique is used to solve Eq. (2) because it is more flexible and is easier to use than an exact solution. Finite difference expressions are used to represent Eq. (2). Gauss-Siedel iteration with under relaxation<sup>11</sup> is used to solve the set of equations. This method was chosen because of its ability to handle ill-conditioned systems of nonlinear equations. The main feature of this technique is the relaxation method. If a system of equations is ill-conditioned, then the most recently calculated values can be modified to prevent divergence. This means the most current values become a weighted average of the relaxation coefficient and the values from the previous iteration. Modifying the most recent values prevents these values from being overestimated for the next iteration.

#### Parameter Estimation

As mentioned earlier, certain parameters describing the radiative field within a sooty pool fire must be determined. Nonlinear parameter estimation is used to link experimental information in the form of radiative heat fluxes and flame temperatures to the analytical model to estimate the absorption coefficient and the extinction coefficient. The following assumptions are made about the measurement errors to develop the maximum likelihood estimator<sup>10</sup>:

1. Additive measurement errors  $\gamma_i = \eta_i + \epsilon_i$
2. Measurement errors have zero mean.
3. Measurement errors are noncorrelated.
4. Measurement errors are normally distributed.
5. The covariance matrix of the measurement errors is known.
6. Independent variables are errorless.
7. Parameters are nonrandom and there is no prior information about them.

Note that these assumptions are not general for the maximum likelihood estimator but are a special case used for this investigation<sup>10</sup>.

Assumption two indicates that the measurement errors are not biased. This indicates the importance of knowing the sources of biased errors so they can be minimized. For this investigation, the correlation between measurement errors was not determined. However, the measurement locations are independent of each other and it was assumed the correlation between measurement errors is small and can be neglected.

With these assumptions the likelihood function in matrix form is:

$$S_{ML} = (\mathbf{Y} - \bar{\eta})^T \bar{\psi}^{-1} (\mathbf{Y} - \bar{\eta}) \quad \text{Eq. (8)}$$

where  $\mathbf{Y}$  represents the experimental data,  $\bar{\eta}$  represents the computed data, and  $\bar{\psi}$  represents the covariance matrix. The diagonal elements of the covariance matrix contain the variance associated with data points.

The parameter estimation method seeks to minimize the likelihood function with respect to the parameters. After performing this differentiation the following is obtained:

$$\bar{V}_B S_{ML} = \bar{X}^T \bar{\psi}^{-1} (\bar{Y} - \bar{\eta}) = 0 \quad \text{Eq. (9)}$$

The new term shown in Eq. (9),  $\bar{X}$ , is called the sensitivity matrix. It is a matrix of derivatives with respect to the parameters. It represents how the analytical model changes with respect to the parameters being estimated.

Since the model is nonlinear with respect to the parameters, the vector that contains the parameters cannot be solved for explicitly, because  $\beta$  appears both implicitly and explicitly in both the model and the sensitivity matrix  $\bar{X}$ . To linearize Eq. (9), a method called the Gauss Method of Minimization will be used<sup>10</sup>. The method uses a Taylor series expansion that neglects higher order terms. Performing a Taylor series expansion on Eq. (9), the maximum likelihood estimator in its final form is

$$\bar{B} = \bar{b} + \bar{P}^{-1} [\bar{X}^T \bar{\psi}^{-1} \{\bar{Y} - \bar{\eta}(\bar{b})\}] \quad \text{Eq. (10)}$$

where

$$\bar{P} = \bar{X}^T \bar{\psi}^{-1} \bar{X} \quad \text{Eq. (11)}$$

$\bar{b}$  represents the vector containing the initial guesses for the parameters.

### Experimentation

In order to quantify the radiative heat transfer parameters shown in Eq. (2), experimental measurements of flame temperature and radiative heat flux were obtained.

A device was initially designed for combustion chamber applications was used to measure the radiative flux within the fire. This marks the first time (to our knowledge) that this type of device was used in pool fire applications. The transpiration radiometer was first developed by Moffat<sup>5</sup>. This device forces a non-participating gas (nitrogen) through a porous material in an amount sufficient to blow off the boundary layer that would otherwise form on the sensing surface of the gage (see Fig. 1). It has been shown by these authors that, with proper design and calibration, the convective heat flux at the sensing surface of the radiometer can be eliminated, leaving only the radiation component of the total heat flux to be measured. For more information on the characterization and operation of the transpiration radiometer, see Ref. 4 and Ref. 5.

The initial construction of the gage was modified to meet the following criteria:

1. Since the entire gage is located directly in the fire, it must be able to withstand temperatures as high as 1200 Kelvin without affecting calibration.
2. Installation of the differential and inner wall thermocouples should not be different.
3. The gage should be small enough so as not to greatly disturb the local fire environment.

The Thermal Test and Analysis group used the Radiant Heat Facility at Sandia National Laboratories to calibrate the transpiration radiometers. To assure that true conditions were maintained during the calibration procedure, the inner wall temperature of the gage was kept at the same level that would be seen in an actual fire. Also the

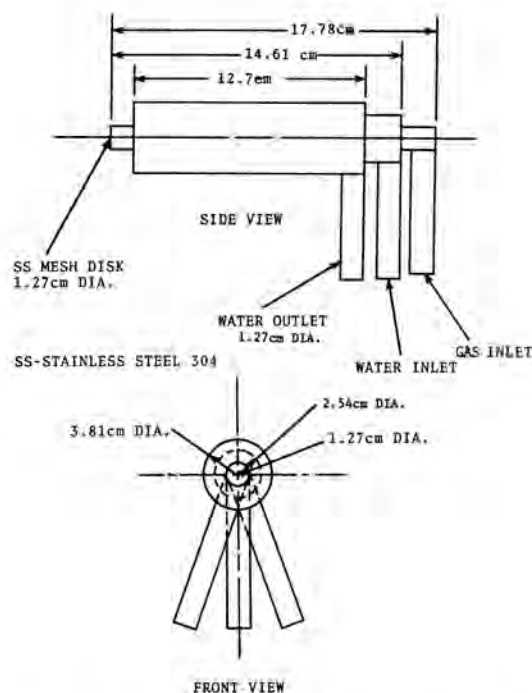


Fig. 1. Modified Transpiration Radiometer

transpiration flow rate was kept at the same level that would be needed for an actual fire test. Basically, the calibration procedure of the transpiration radiometer was the same as that suggested by Moffat<sup>5</sup>. The spectral distribution of the incident radiation from the pool fire was unknown prior to the fire test. Although exact fire conditions could not be reproduced during calibration, every measure was taken to assure proper calibration for pool fire conditions. One must realize that the calibration is accurate only for test conditions where diffuse uniform radiative flux is incident on the sensing surface of the radiometer. During the characterization process it was demonstrated the transpiration radiometer would be very useful for fire applications. The main properties of the transpiration radiometer can be stated as follows:

1. The results obtained from the transpiration radiometer are repeatable and stable.
2. The transpiration radiometer is a sturdy device that can be used in a fire environment.
3. A transpiration flow rate of approximately  $0.438 \times 10^{-3}$  scms will eliminate the convection effects of a fire with an upward velocity of 4.57 meters per second or less and eliminate soot buildup on the sensing surface.
4. A 99% of full-scale response time of approximately 2.5 seconds was observed.

### Fire Testing at Sandia

On September 1st, 1984, a large-scale pool fire test was run by the Thermal Test and Analysis group of Sandia National Laboratories. The fire test was run in the Sandia Large-Scale Pool Fire Test Facility which consists of a 9.14 x 18.29 meter pool and a supporting data acquisition system. Within the pool, a layer of liquid JP-4 jet fuel is floated on top of water. Figure (2) shows the test pool.

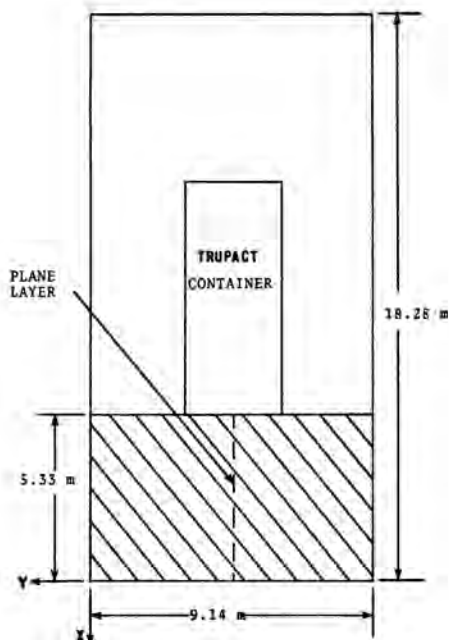


Fig. 2. 9.14 m x 18.29 m Test Pool

During the fire test, the 5.334 x 9.144 meter cross-hatched section shown was assigned specifically for fire characterization sensors, which included transpiration radiometers and flame thermocouples. Practical considerations and constraints had to be considered when determining where to place the sensors within the cross-hatched section. Equation (2) requires a one-dimensional plane layer geometry. Figure (2) shows two possible directions, x and y. From previous experiments run by Sandia National Laboratories<sup>12</sup>, wind conditions were more severe in the y direction; therefore, the x direction was chosen to represent the plane layer. For symmetry reasons, the plane layer was located in the center of the 9.144 meter length.

Six transpiration radiometers were used in the large-scale pool fire test. Two of the six gages were used to measure the boundary flux at  $x=0$  and at  $x=l$ . The  $x=0$  location was located as close as possible to the large test item (TRUPACT). The supporting lines for transpiration gas, cooling water, and the length of the gage required the sensing plane of the transpiration gage be located 0.381 meters from the large test item. At the  $x=l$  boundary, the same 0.381-meter distance was used. This left 4.572 meters in which to place two more measurement locations. For symmetry reasons, the two interior measurement locations were spaced evenly apart.

Figure (3) shows the positioning of the four measurement locations. The distance between each measurement location or measurement plane was approximately 152.4 centimeters. For each of the two interior measurement locations, the sensors were positioned approximately 20.32 centimeters apart. The distance from the initial fuel level to the centerline of the sensing surface of each radiometer was approximately 124.46 centimeters.

Each of the two center measurement locations consisted of two transpiration radiometers. One radiometer looked into the fire towards the TRUPACT test article measuring the  $q^+$  radiative flux. The sensing surface of the other radiometer was oriented 180 degrees from the other radiometer looking out towards the fire boundary measuring the  $q^+$  radiative

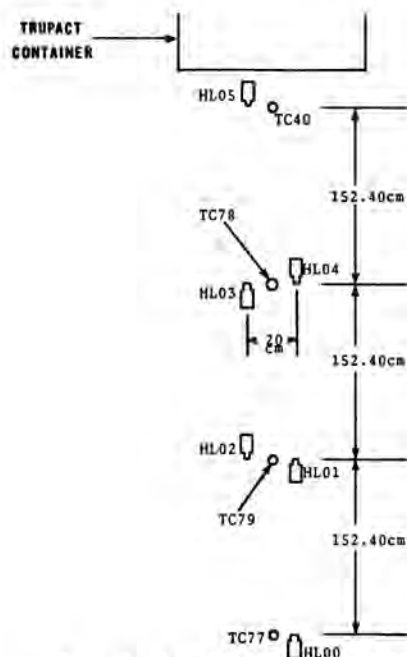


Fig. 3. Final Placement of Transducers

flux. The boundary measurement location at  $x=0.0$  consist of one transpiration radiometer looking into the fire measuring  $q^-$ , and one flame thermocouple. The boundary measurement location at  $x=l$  consisted of one transpiration radiometer looking into the fire measuring  $q^+$ , and one flame thermocouple.

At each measurement location, there was one flame thermocouple located in the same plane as the transpiration radiometer sensing surface. Type K thermocouple wire was used for this application. The thermocouple junction was not shielded and interacted with the convective and radiative heat flux within the fire. Soot buildup on the bare thermocouple junction was not a problem. It has been indicated by Mata<sup>13</sup> that at flame temperatures of approximately 700 degrees Kelvin, soot deposits begin to burn off. At flame temperatures above 700 degrees Kelvin, soot deposits do not form.

Figure (4) shows a gage before being wrapped with Fiberfrax Durablanket Insulation<sup>14</sup>. There are three support lines for each gage. Two lines are used for cooling water in and cooling water out. The third line provides the nitrogen transpiration gas. Figure (5) shows a close-up of the gage after being insulated with Fiberfrax insulation. The gage is wrapped with approximately 1.3-centimeters-thick insulation on all surfaces except the sensing surface.

## RESULTS

For the fire test period of 21 minutes to 32 minutes, three quasi-steady time intervals were investigated. A quasi-steady time interval is defined in Reference 8 as being "from a practical standpoint, the temporal means of certain flame properties can be considered essentially invariant with time." The quasi-steady regions were determined based on these criteria:

1. All data channels should be physically consistent with one another.
2. The intervals must have a relatively small standard deviation about the sample mean.



Fig. 4. Photograph of Transpiration Radiometers Before Insulation



Fig. 5. Photograph of Transpiration Radiometers Following Insulation with Fiberfrax

The length of the time intervals range from 18 seconds to 28 seconds. The values in the quasi-steady regions must be averaged over time to determine the sample mean, which is an estimate of the true value of the fire conditions (flame temperatures and radiative fluxes) that exist in the time intervals.

The mean values of flame temperatures and radiative heat fluxes with corresponding one sigma standard deviations obtained from each quasi-steady time interval are shown in Tables I and II. The percent standard deviation for temperature range from 2 to 9 percent and that for radiative fluxes range from 5 to 40 percent. Reference (8) indicates the average percentage standard deviations for temperature are 6 percent and for radiant fluxes are 30 percent.

#### Results Obtained From Parameter Estimation

Parameter estimation, as previously described was used to link experimental information with the theoretical model in an effort to estimate the absorption coefficient and extinction coefficient.

TABLE I

Mean Flame Temperatures with Corresponding One Sigma Standard Deviations at Each Quasi-Steady Time Interval

TIME PERIOD	THERMOCOUPLE	FLAME TEMPERATURE (DEG K)	s ( $1\sigma$ ) (DEG K)
24 MIN	TC40	1052.63	+/- 23.18
24 MIN	TC77	693.21	+/- 35.31
24 MIN	TC78	1146.43	+/- 62.41
24 MIN	TC79	1270.93	+/- 61.87
27 MIN	TC40	998.07	+/- 6.36
27 MIN	TC77	663.67	+/- 31.20
27 MIN	TC78	1128.34	+/- 31.38
27 MIN	TC79	1175.41	+/-101.14
28 MIN	TC40	1014.52	+/- 9.39
28 MIN	TC77	689.41	+/- 25.37
28 MIN	TC78	1255.25	+/- 44.82
28 MIN	TC79	1097.22	+/- 66.03

TABLE II

Mean Radiative Fluxes with Corresponding One Sigma Standard Deviations for the 24- and 27- and 28-Minute Quasi-Steady Time Intervals

TIME PERIOD	RADIOMETER	RADIATIVE HEAT FLUX (W/cm <sup>2</sup> )	s ( $1\sigma$ ) (W/cm <sup>2</sup> )
24 MIN	HLO0	11.56	+/-0.59
24 MIN	HLO1	15.94	+/-1.91
24 MIN	HLO2	12.91	+/-1.11
24 MIN	HLO3	8.08	+/-1.38
24 MIN	HLO4	8.29	+/-2.41
24 MIN	HLO5	6.70	+/-1.00
27 MIN	HLO0	6.22	+/-0.87
27 MIN	HLO1	14.36	+/-1.08
27 MIN	HLO2	10.56	+/-1.84
27 MIN	HLO3	8.76	+/-2.05
27 MIN	HLO4	9.52	+/-2.58
27 MIN	HLO5	7.69	+/-0.95
28 MIN	HLO0	5.94	+/-2.21
28 MIN	HLO1	9.85	+/-1.59
28 MIN	HLO2	10.61	+/-1.67
28 MIN	HLO3	8.43	+/-1.38
28 MIN	HLO4	10.61	+/-2.29
28 MIN	HLO5	8.79	+/-3.64

Only three out of four measurement locations could be used for parameter estimation. Initially, all four measurement locations were used, but this led to large errors in the estimated parameters. Experimental data (radiative fluxes and flame temperatures) obtained from the fire test indicated that the TRUPACT container altered the local fire environment. Therefore the radiation field did not follow the approximations inherent in the model. This change in the fire environment was not taken into account in the model.

Since the model cannot distinguish between the forward-moving flux field,  $q^+$ , and the backward-moving flux field  $q^-$ , it was attempted to estimate two sets of parameter estimates.

During this analysis, it was determined that both the absorption and extinction coefficients could not be estimated simultaneously<sup>4</sup>. The justifications for this are lack of information, the fire is absorption dominant, and the parameters are linearly dependent. Therefore, the extinction coefficient was simplified to a mean absorption coefficient by neglecting isotropic scattering and the model simplifies to a one parameter model. From Mie theory<sup>6</sup>

the scattering cross section depends on the relationship  $\pi D/\lambda^4$ , and the absorption cross section depends on  $\pi D/\lambda$ . The radiation from soot particles in a flame is usually concentrated in the visible and infrared region of the spectrum. With very small soot particles (average diameter of soot particle) there is a small contribution of emitted energy in the infrared region. In this case, the scattering cross section is less than one and absorption becomes dominant and scattering can be neglected. Felske and Tien<sup>15</sup>, make the same assumptions about the scattering contribution of soot particles and go further to state that in large scale pool fires, soot emission dominates gas species emission, therefore justifying the non-scattering assumption. Their analysis illustrates the relative importance of gas and soot emission under typical flame conditions<sup>15</sup>. They indicate that for a large volume fraction of soot, the emission of the fire (which includes banded gas emission and soot emission) is completely dominated by soot emission. The results of the large-scale pool fire indicated large soot concentrations at temperatures in the region of 1000 Kelvin. Felske and Tien state that "at temperatures of 1000 K, where the maximum of the Planck function occurs at about 2.9  $\mu$ m, any increase in temperature will shift the blackbody weighting curve away from the region of strong gaseous emission toward the region of strong soot emission."

The errors in temperature measurements, and having run only one fire test, led to no conclusion about scattering. However, the work done by Felske and Tien<sup>15</sup> was considered and the scattering contribution was neglected. The results from the one parameter model are shown in Tables III and IV.

TABLE III

Estimated Absorption Coefficient Obtained From  $q_t$  Measurements

TIME INTERVAL (MIN)	$\alpha(1/cm)$
24	0.0069 +/- 0.0027
27	0.0081 +/- 0.0027
28	0.0062 +/- 0.0055

TABLE IV

Estimated Absorption Coefficients Obtained From  $q -$  Measurements

TIME INTERVAL (MIN)	$\alpha(1/cm)$
24	0.0175 +/- 0.0113
27	N/A
28	0.0119 +/- 0.0166

De Ris<sup>1</sup> shows similar results obtained from the combustion of polystyrene (PS), polypropylene (PP), and polymethylmethacrylate (PMMA). The results are shown below:

TABLE V

Absorption Coefficients Determined by De Ris

FUEL TYPE	$\alpha(1/cm)$
PS	0.053
PP	0.018
PMMA	0.013

Also, Markstein<sup>16</sup> presents results obtained from the combustion of PMMA. Markstein indicates a maximum absorption coefficient of 0.0136/cm. Atallah and Raj<sup>9</sup> indicate a mean absorption coefficient of 0.005/cm from the combustion of LNG fires. Also, Orloff<sup>17</sup> indicates an absorption coefficient of 0.015/cm for PMMA.

### Discussion of Errors

There are many forms of errors associated with the measurements of flame temperatures and radiative heat fluxes. Among the most important are

1. biased errors,
2. errors in the independent variables,
3. random errors.

Knowledge of errors in temperature measurements are very important. The model contains a source term ( $\sigma T^4$ ) in which flame temperatures are raised to the fourth power. Any errors in the temperature measurements will cause large errors in the parameter estimates. It was shown<sup>4</sup> that biased flame temperature errors had a great effect on parameter estimates. In the case where temperatures were biased independently of flux, the largest percent difference between the original parameter estimate and the biased parameter estimate was approximately 66 percent<sup>4</sup>. At some fire, time intervals, a ten-percent bias would not allow parameter estimates to be obtained<sup>4</sup>. Then, the temperature and flux values were biased simultaneously. The largest percent difference between the original parameter estimate and the biased parameter estimate was approximately 62 percent<sup>4</sup>.

By biasing temperatures and radiative fluxes independently, one can determine which errors are more important. Biasing radiative flux measurements independent of temperature measurements produced percent differences as large as 28 percent,<sup>4</sup> indicating that biased flux measurements are not as important as biased temperature measurements.

In this research work, it was assumed that biased errors were not present. The validity of this assumption could not be verified because of the lack of experimental information. However, there are several sources of biased errors that should be considered in further research.

Biased errors associated with transducers can be reduced by repositioning them after each test. Biased errors associated with the cold fuel surface of the fire can be reduced or eliminated by proper positioning of the transducers. Also, to improve the statistics of the experiment, more controlled tests and more tests are required.

It was also shown<sup>4</sup> that measurement errors (which include errors associated with the data acquisition system, errors associated with the conversion of voltages to temperatures, and errors associated with the natural fluctuation of the fire) were not as important to parameter estimates as they were to the one-sigma error of the parameter estimates. For the case of an additional ten-percent measurement error, the parameter estimates were not affected. Only the one-sigma error of the parameter estimate increased or decreased. These results are important to fire research because of the constantly changing fire environment.

Because the flame thermocouple junction is interacting with both the convective and radiative fire environment, one must ask what temperature is being measured. The estimated mean absorption coefficients indicate that the fire is optically thick. This means that the radiative contribution from other portions of the fire outside of the optically thick region will be small. Therefore, the local environment surrounding the thermocouple junction can be assumed isothermal, and the local convection and radiation temperatures are approximately the same.

Another source of error when considering flame temperature measurements is that due to soot buildup on the thermocouple junction. Any soot buildup on the junction will affect the accuracy of the calibration. This problem was considered earlier and Mata<sup>13</sup> stated that soot deposits start to burn off thermocouple junctions at flame temperatures above 700 Kelvin. One thermocouple junction indicated temperatures below 700 Kelvin. In this investigation this type of error was not considered but one should realize that it exists.

Errors in the radiative flux measurements are of the same form as the temperature measurements. It was shown<sup>4</sup> that biased errors in the flux measurements changed estimated absorption coefficients by as much as 28 percent. These results are not as drastic as those obtained from biased temperature measurements, but large differences in the parameter estimates still result.

Before ending the discussion of errors, it should be noted that errors in the independent variables such as spatial location were not considered in this investigation. In future analysis, it is recommended that these types of errors be considered.

#### CONCLUSIONS

In this work it was determined that scattering information could not be obtained with the given experimental information. The main reasons that scattering information could not be obtained are these:

1. The relative closeness of the absorption coefficient and the extinction coefficient, estimated from the model which corresponds to the literature accepted view that the pool fire is absorption dominated.
2. The presence of the TRUPACT container which altered the local fire environment, causing errors in the flame temperature measurements and the radiative heat flux measurements.
3. The lack of experimental information.

The end result of this analysis provides a method of estimating mean flame absorption coefficients, given flame temperature distributions and radiative flux distributions. Estimated absorption coefficients obtained from this work have compared to those presented by Reference 1, 16, and 17. The estimated absorption coefficients along with the experimentally determined flame temperatures and heat fluxes can be used when analysing casks engulfed within large-scale soot pool fires.

This method that estimates mean absorption coefficients is very sensitive to measurement errors. In further analysis, it is recommended that more tests be run under more controlled conditions. This will improve the statistical control of the

data for parameter estimation. To reduce biased errors, transducers should be relocated as often as possible.

The transpiration radiometer, used within the sooty pool fire to measure radiative heat fluxes, performed well. Further work needs to be done to improve the sensitivity of the radiometer.

#### REFERENCES

1. De Ris, J.: "Fire Radiation-A Review," 17th Symposium (Int.) on Combustion, 1003-1016, 1978.
2. Birk, A. M. and Oosthuizen, P. H.: "Model for the Prediction of Radiant Heat Transfer to a Horizontal Cylinder Engulfed in Flames," Paper No. 82-WA/HT-52, 1982.
3. Pagni, P. J. and Bard, S.: "Particulate Volume Fractions in Diffusion Flames," 17th Symposium (Int.) on Combustion, 1017-1028, 1978.
4. Longenbaugh, R. S. and Matthews, L. K.: "Experimental and Theoretical Analysis of the Radiative Transfer Inside of a Sooty Pool Fire," SAND85-0123, to be released.
5. Moffat, R. J. et al.: "Development of a Transpiration Radiometer," Instrument Society of America, Conference Proceedings, Paper No. 613, 1971.
6. Siegel, R. and Howell, J. R.: Thermal Radiation Heat Transfer, McGraw Hill Book Company, New York, N.Y., 1972.
7. Code of Federal Regulations 10 Energy Parts 0 to 199 (10 CFR 71) US Government Printing Office, Washington, 1980.
8. Russell, L. H. and Canfield, J. A.: "Experimental Measurement of Heat Transfer to a Cylinder Immersed in a Large Aviation-Fuel Fire," ASME Paper No. 73-HT-2, 1973.
9. Atallah, S. and Raj, P.: "Thermal Radiation From LNG Spill Fires," Arthur D. Little, Inc., 1971.
10. Beck, J. V. and Arnold, K. J.: Parameter Estimation in Engineering and Science, John Wiley & Sons, Inc., New York, N.Y., 1977.
11. Hornbeck, R. W.: Numerical Methods, Quantum Publishers, Inc., New York, N.Y., 1975.
12. Neff, J. J., Keltner, N. and Mata, R.: "Thermal Measurements in a Series of Large Pool Fires," SAND85-0196, to be released.
13. Mata, R.: "Personal Communications in Regards to Large-Scale Sooty Pool Fires," Sandia Laboratories Division 7537, 1984.
14. Fiberfrax Durablanket Insulation: The Carborundum Company, Insulation Division, Niagara Falls, New York, N.Y., 1983.
15. Felske, J. D. and Tien, C. L.: "Calculation of the Emissivity of Luminous Flames," *Combustion Science and Technology*, 1973, 7, 25-31.
16. Markstein, G. H.: "Scanning-Radiometer Measurements of the Radiance Distribution in PMMA Pool Fires," Eighteenth Symposium on Combustion, The Combustion Institute, 1981.

17. Orloff, L.: "Simplified Radiation Modeling of Pool Fires," 18th Symposium (Int.) on Combustion, 549-561, 1981.

NOMENCLATURE

$\bar{b}$	parameter vector (initial guess)
$D$	mean diameter of soot particles
$E_b$	blackbody emissive power
$I$	intensity of thermal radiation
$I_0$	intensity at boundary = 0
$I_b$	blackbody intensity
$L$	likelihood function
ML	maximum likelihood estimator used in parameter estimation
$n$	index of refraction or number of observations or degrees of freedom
OLS	ordinary least squares estimator used in parameter estimation
$\bar{P}$	the P matrix containing $\bar{x}^T \bar{\psi}^{-1} \bar{x}$
$q$	net radiative flux
$q^+$	radiative flux in the forward moving direction
$q^-$	radiative flux in the backward moving direction
$s$	standard deviation of the sample mean
$s^2$	variance of the sample mean
$S_{ML}$	maximum likelihood estimator used in parameter estimation
$S_{LS}$	least-squares estimator used in parameter estimation
$T$	temperature
$\bar{x}$	sensitivity coefficient

$x$	spatial dimension
$\bar{Y}$	vector containing experimental data (radiative flux measurements)
$Y_i$	experimental data

Greek Symbols

$\alpha$	total hemispherical absorption coefficient or the thermal diffusivity of the Sandia calorimeter
$\beta$	parameter
$\bar{\beta}$	parameter vector
$\nabla$	del operator with respect to the parameter $\beta$
$l$	logarithm of the likelihood function or thickness of a plane layer
$\sigma_s$	scattering coefficient
$\sigma$	Boltzman constant or one sigma standard deviation of measurements
$\phi$	angle of scattered radiation in direction of travel
$\phi'$	angle of scattered radiation from some other direction other than the direction of travel
$\Phi$	scattering phase function
$\mu$	directional cosine
$\tau$	optical thickness
$\eta_1$	computed data
$\bar{\eta}$	vector of computed data
$\Psi$	covariance matrix containing measurement errors
$\kappa$	extinction coefficient
$\epsilon_1$	error associated with experimental measurements
$\lambda$	wavelength